

# Extended chain crystal growth of low molecular mass poly(ethylene oxide) and $\alpha,\omega$ -methoxy poly(ethylene oxide) fractions near their melting temperatures

Stephen Z. D. Cheng\*, Jianhua Chen and Daniel P. Heberer

*Institute and Department of Polymer Science, College of Polymer Science and Polymer Engineering, The University of Akron, Akron, OH 44325-3909, USA*

*(Received 22 January 1991; revised 26 March 1991; accepted 30 March 1991)*

For low molecular mass poly(ethylene oxide) (PEO) and  $\alpha,\omega$ -methoxy poly(ethylene oxide) (MPEO) fractions, extended chain crystals can grow when isothermal crystallization temperatures are near their melting temperatures (supercooling  $\Delta T = T_m - T_c$  is in the range of a few degrees). Experimentally, observed lamellar thicknesses of the extended chain crystals are constants in this supercooling region. Linear relationships between crystal growth rate ( $G$ ) and supercooling ( $\Delta T$ ) can be observed. Absolute values of the slopes of these relationships decrease with increasing molecular length. Additionally, MPEO fractions generally have higher slope values when compared with their PEO counterparts. Nevertheless, this difference between PEO and MPEO fractions gradually vanishes with increasing molecular length. Extended chain single lamellar crystals are highly faceted in these temperature regions, and their aspect ratios vary with supercooling as well as molecular length. Nucleation theory for the growth of extended chain crystals is applied. The transient chain-end surface free energy,  $\sigma'$ , and the lateral surface free energy,  $\sigma$ , for the PEO and MPEO fractions possess entropic origins. The rough surface growth model is also discussed.

**(Keywords: extended chain crystal; linear crystal growth rate; low molecular mass fraction; molecular length; morphology; nucleation theory; poly(ethylene oxide); single lamellar crystal; transient surface free energy)**

## INTRODUCTION

Single lamellar crystals of low molecular mass poly(ethylene oxide) (PEO) fractions grown from the melt have been observed since the early 1970s beginning with the pioneering work of Kovacs *et al.*<sup>1-5</sup>. The linear crystal growth, crystal melting and isothermal thickening behaviour of these fractions have been extensively studied. The most important discovery was the recognition that chains integrally fold when incorporated into crystals, as evidenced by quantized changes of the lamellar thickness with varying crystallization conditions<sup>1-5</sup>. In concurrence with this, for extended chain crystal growth, a linear decrease of crystal growth rate ( $G$ ) with supercooling ( $\Delta T$ ) was observed<sup>1-6</sup>.

Recently, we studied crystallization behaviour of low molecular mass PEO fractions with different end groups (hydroxyl and methoxy groups, MPEO). Transient non-integral folding chain crystal growth was observed over a wide crystallization temperature region, and similar linear relationships between  $G$  and  $\Delta T$  for extended chain crystal growth in these fractions were also found<sup>7-10</sup>. In fact, these kinds of relationships are not unique to low molecular mass PEO fractions. In 1985, Hoffman<sup>11</sup> reported the same phenomenon in highly purified  $n$ -C<sub>94</sub>H<sub>190</sub>. Similar observations were also found in a polyethylene (PE) fraction (C<sub>207</sub>H<sub>416</sub>, polydispersity = 1.07) for extended chain crystals grown from solution<sup>12-14</sup>.

After the report of experimental data on linear crystal growth rates of low molecular mass PEO fractions<sup>1-5</sup>, it was found that the lateral surface free energy,  $\sigma$ , for the extended chain crystals at least, was far too small to be credible, and apparently acted as if it were strongly dependent upon the molecular length. This led to the conclusion that the current theories of polymer crystal growth<sup>15-19</sup> were seriously flawed in the case of low molecular mass oligomers and fractions. The flaws were due to the failure of the basic postulates resulting in an incorrect evaluation of the nucleation barrier and/or an assumption of the sequential deposition of the consecutive stems of fixed length<sup>20</sup>. On the other hand, Hoffman successfully applied the nucleation theory to explain the integral folding chain crystals in low molecular mass PEO fractions<sup>21</sup>. For the linear relationships between crystal growth rate ( $G$ ) of extended chain crystals and supercooling ( $\Delta T$ ) in low molecular mass pure oligomers and fractions, Hoffman<sup>11</sup> further suggested a treatment to explain the experimental data obtained for an  $n$ -C<sub>94</sub>H<sub>190</sub> and a fraction of C<sub>207</sub>H<sub>416</sub>. A constant lateral surface free energy, close to that found for folded chain crystals in polyethylene (PE) was obtained. Recently, a detailed description based on nucleation theory has been proposed to illustrate the crystal growth behaviour of extended chain crystals. It includes both a linear relationship between  $G$  and  $\Delta T$ <sup>11-14</sup> during folded chain to extended chain crystal transitions<sup>22</sup>, as well as retardation of the crystal growth<sup>23,24</sup>. In an alternative approach Sadler described these linear relationships

\*To whom correspondence should be addressed

between  $G$  and  $\Delta T$  in low molecular mass PEO fractions through a rough surface growth model<sup>6</sup>.

In this paper, special attention is paid to the extended chain crystal growth of low molecular mass PEO and MPEO fractions near their melting temperatures. Specifically, supercooling  $\Delta T = T_m - T_c$  is small, generally in the range of a few degrees. With increasing molecular length the supercooling range, where extended chain crystals grow, narrows<sup>1-5</sup>. The linear crystal growth rates along different crystallographic planes can be measured by polarized light microscopy (PLM) and application of a 'self-seeding' technique<sup>1</sup>. In order to make a systematic study of the extended chain crystal growth behaviour, we have measured linear crystal growth rates for both PEO and MPEO fractions. By comparing the growth rates for specimens having the same molecular lengths but different end groups, and for specimens having different molecular lengths yet the same end group, nucleation theory is tested. The difference between the nucleation and the rough surface growth models is also discussed.

## EXPERIMENTAL

### Materials

The PEO fractions were purchased from Polymer Laboratories and refractionated in our laboratory. In this paper, three molecular mass fractions were used: PEO (MW = 3000), PEO (MW = 4250) and PEO (MW = 7100), with polydispersities of 1.02–1.04. The PEO fractions were also methoxylated by the method of Cooper and Booth<sup>25</sup>. The detailed procedures have been described in a previous publication<sup>9</sup>. The molecular mass and molecular mass distribution were essentially unchanged by the methoxylation process. Infra red (i.r.) spectroscopy was used to confirm the conversion of the hydroxyl end group to a methoxy one. I.r. results showed a conversion of about  $98 \pm 1\%$ . The elemental analysis found no residual iodine content (i.e. below detectable limits).

### Instrumentation and experiments

During crystallization of PEO and MPEO fractions, the self-seeding technique reported by Kovacs and Gonthier<sup>1</sup> was adopted. Samples were heated to 30 K above their melting temperatures under a dry nitrogen atmosphere, then cooled to 318.2 K, where crystallization occurs rapidly. The specimens were reheated at  $0.1 \text{ K min}^{-1}$  in a reproducible manner to a temperature  $T_s = T_m - 0.5 \text{ K}$ . At this temperature the major portion of the PEO or MPEO materials melt, although often slowly. The remaining unmelted solid seeds represent a volume fraction on the order of 0.001% or less. The specimens were kept isothermally at  $T_s$  for 25 min then

**Table 1** Melting temperatures of extended chain single lamellar crystals of different molecular mass PEO and MPEO fractions

Molecular mass	Average chain length (nm)	$T_m$ (K)
PEO (3000)	18.9	331.9
MPEO (3000)	19.0	332.5
PEO (4250)	26.9	334.3
MPEO (4250)	27.0	334.8
PEO (7100)	44.9	337.2
MPEO (7100)	45.0	337.4

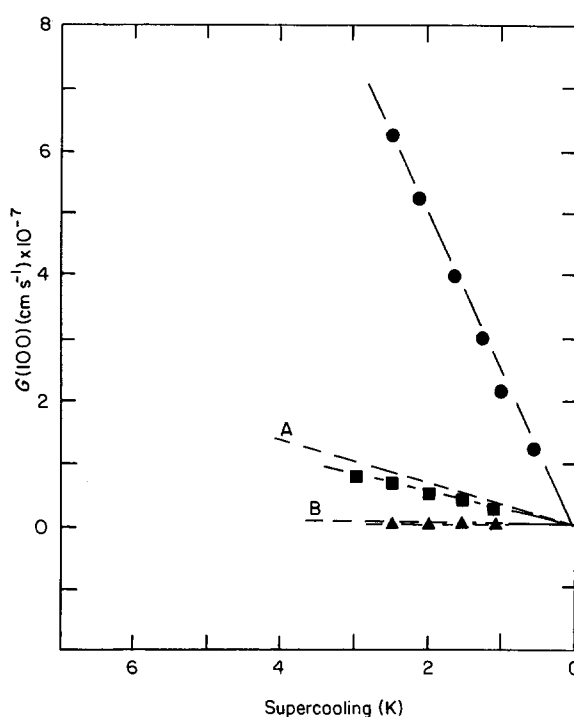


**Figure 1** Relationships between linear crystal growth rate ( $G$ ) along (1 0 0) crystallographic planes and supercooling ( $\Delta T$ ) for: ●, PEO (MW = 3000); ■, PEO (MW = 4250); ▲, PEO (MW = 7100) fractions. Data reported by Kovacs *et al.*<sup>1-5</sup> is shown for: A, PEO (MW = 3900); B, PEO (MW = 5970) fractions

quickly cooled to preset crystallization temperatures. *Table 1* lists melting temperatures of these PEO and MPEO fractions.

A polarized light microscope (Nikon Labophoto-pol) was used. The specimens were crystallized in an oil bath (Neslab TMV-40DD) under dry nitrogen atmosphere. After a given crystallization time, the specimens were quenched into a dry ice and acetone mixture ( $T_q = 195.2 \text{ K}$ ). The rationale for using this process is that one cannot observe any birefringence difference for single lamellar crystals because the chain direction is parallel to the light direction. During the quench from  $T_c$  to  $T_q$ , each active site on the crystals which can initiate growth is decorated by tiny, highly contrasting, optically birefringent spherulites which have a typical diameter of  $3-5 \mu\text{m}$ . Since the lateral surface of the crystalline lamellae grown at  $T_c$  offers a number of active sites along the crystal edges, quenching thereby produces a decorative layer around the free edges of the single crystals, provided that they were originally surrounded by molten chain molecules.

## RESULTS

### Crystal growth rates of extended chain crystals

*Figure 1* shows relationships between linear crystal growth rates ( $G$ ) and supercooling ( $\Delta T$ ) for three PEO fractions with different molecular masses: 3000, 4250 and 7100. The data for the PEO (MW = 3000) fraction introduced in this work have been reported previously<sup>10</sup>. These growth rates were measured by following the direction of fastest growth of the crystallographic planes, in particular, along the (1 0 0) planes (see below). For these fractions it is evident that the extended chain crystal growth rates decrease linearly with supercooling.

**Table 2** Slopes of linear relationships between crystal growth rate and supercooling for extended chain crystal growth of different molecular mass PEO and MPEO fractions

Molecular mass	Slope of PEO (cm (s K) <sup>-1</sup> )	Slope of MPEO (cm (s K) <sup>-1</sup> )
3000	$2.53 \times 10^{-7}$	$4.70 \times 10^{-7}$
3900 <sup>a</sup>	$0.32 \times 10^{-7}$	—
4250	$0.28 \times 10^{-7}$	$0.43 \times 10^{-7}$
5970 <sup>a</sup>	$0.29 \times 10^{-8}$	—
7100	$0.50 \times 10^{-9}$	$0.53 \times 10^{-9}$
7760 <sup>a</sup>	$0.40 \times 10^{-9}$	—

<sup>a</sup> Values of slopes of these PEO fractions were obtained by calculating the data from Figure 10 in ref. 3

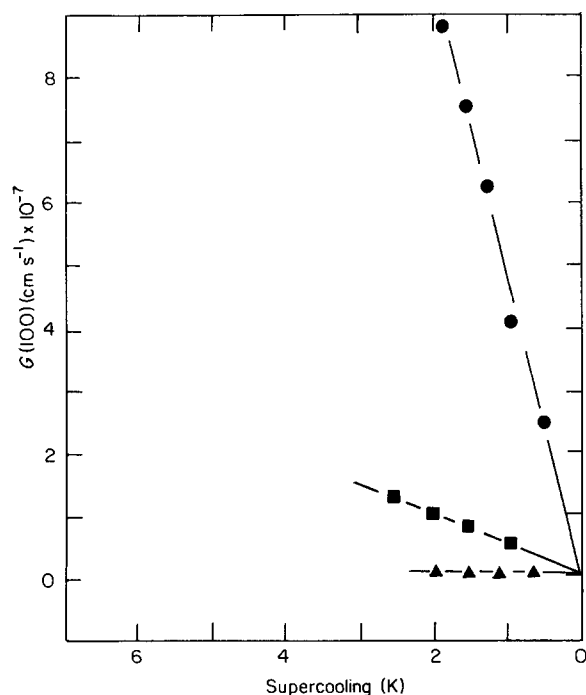


**Figure 2** Relationship between linear crystal growth rate ( $G$ ) along (100) crystallographic planes and supercooling ( $\Delta T$ ) for: ●, MPEO (MW = 3000); ■, MPEO (MW = 4250); ▲, MPEO (MW = 7100) fractions

Furthermore, absolute values of the slopes shown in Figure 1 diminish with increasing molecular length; values are listed in Table 2.

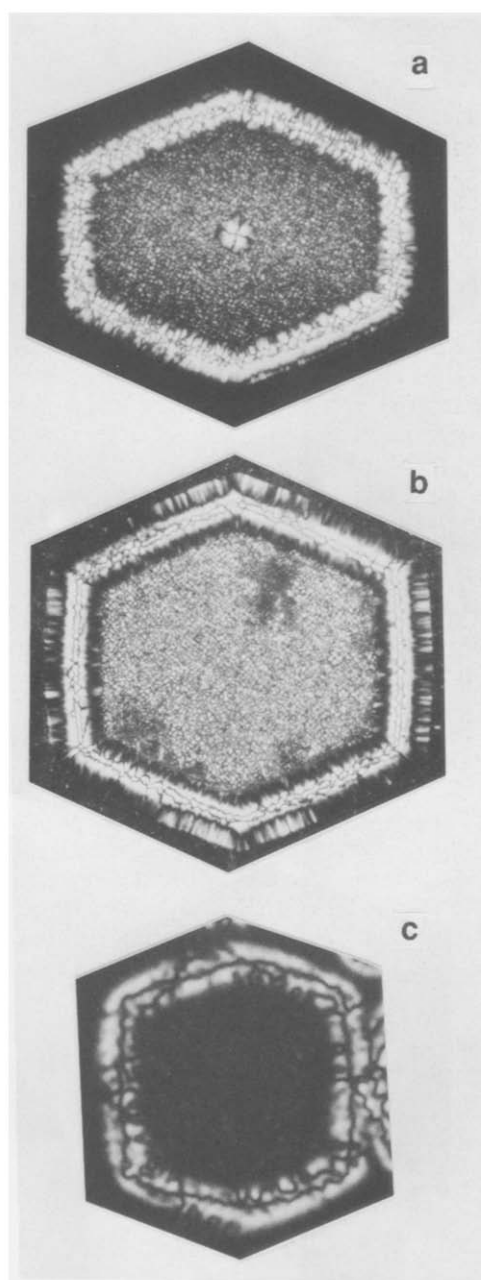
For MPEO fractions, similar situations can be observed as shown in Figure 2. Data for the MPEO (MW = 3000) fraction are from ref. 10. Absolute values of the slopes of these linear relationships between  $G$  and  $\Delta T$  are also given in Table 2. One can clearly see that for the same molecular length, the slope of such a relationship with methoxy end groups is always steeper than its counterpart with hydroxyl end groups. For example, the slope for MPEO (MW = 3000) has an absolute value of  $4.70 \times 10^{-7}$  cm (s K)<sup>-1</sup>, and is 1.86 times higher than that for PEO (MW = 3000). With increasing molecular length, the difference between slopes of the PEO and MPEO fractions with the same molecular length decreases, as shown in Table 2. For MW = 7100, the ratio of MPEO to PEO slopes is only 1.05.

Figure 1 also shows a plot of the crystal growth rate data of extended chain crystals with different molecular mass PEO fractions reported by Kovacs *et al.*<sup>1-5</sup>. It is found that their data also show linear relationships between  $G$

and  $\Delta T$ . The data from our group can be fitted well to the data of Kovacs *et al.* in terms of molecular length sequence. The slopes of their data are also included in Table 2.

#### Crystal morphologies of extended chain crystals

Figures 3a to c are the single lamellar morphologies of extended chain crystals for three different molecular mass PEO fractions at supercoolings of 3.5 K, 2.6 K and 2 K, respectively. All the single lamellar crystals show four {140} and two (100) crystallographic planes. We employ the concept of an aspect ratio as proposed by Kovacs *et al.*<sup>1-5</sup>.  $W$  represents the orthogonal distance between two (100) crystallographic planes and  $H$  indicates the distance between two diagonal tips formed by {140} crystallographic planes in the direction perpendicular to  $W$ . It is interesting that in the temperature region of the extended chain crystal formation the aspect ratio may change with supercooling for each fraction. On the other



**Figure 3** Extended chain single lamellar crystals of PEO fractions crystallized at supercoolings of: (a) 3.5 K for PEO (MW = 3000); (b) 2.6 K for PEO (MW = 4250); (c) 2 K for PEO (MW = 7100)

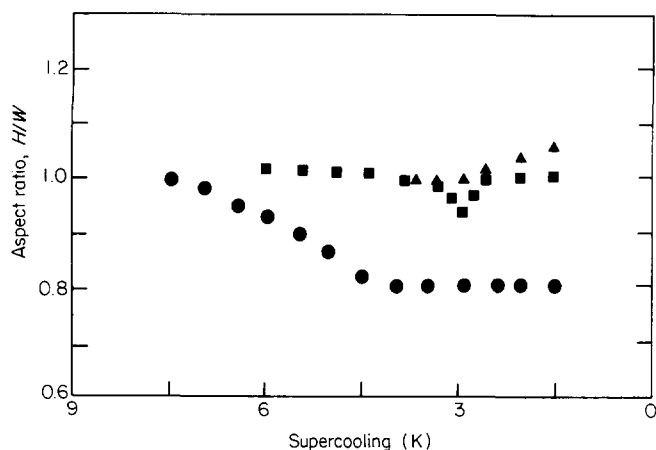


**Figure 4** Changes in aspect ratios ( $H/W$ ) with respect to supercooling of extended chain single lamellar crystals: ●, PEO(MW = 3000); ■, PEO(MW = 4250); ▲, PEO(MW = 7100)

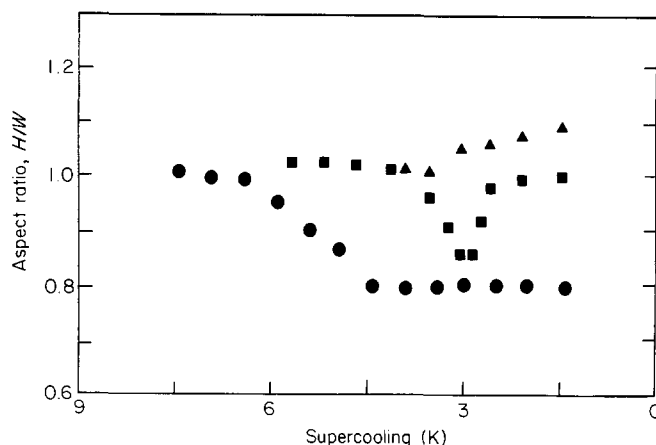


**Figure 6** Changes in aspect ratios ( $H/W$ ) with respect to supercooling of extended chain single lamellar crystals: ●, MPEO(MW = 3000); ■, MPEO(MW = 4250); ▲, MPEO(MW = 7100)

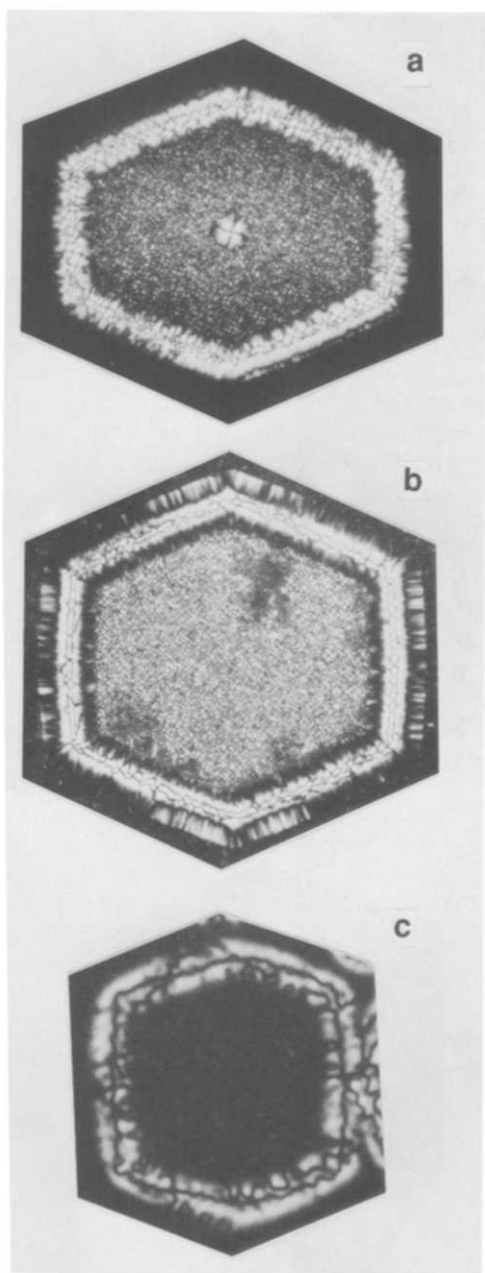


**Figure 5** Extended chain single lamellar crystals of MPEO fractions crystallized at supercoolings of: (a) 3.5 K for MPEO(MW = 3000); (b) 2.6 K for MPEO(MW = 4250); (c) 2 K for MPEO(MW = 7100)

hand, the aspect ratio also varies with molecular length, as shown in *Figure 4*. For example, the aspect ratio of PEO(MW = 3000) fraction remains at 0.80 in this supercooling region. For PEO(MW = 4250) and PEO(MW = 7100), the aspect ratios are in the vicinity of 1.00. For MPEO fractions, similar morphological observations can be obtained as shown in *Figures 5a to c*. *Figure 6* illustrates changes of the aspect ratios of the fractions with supercooling.

It should be pointed out that *Figures 3a to c* and *Figures 5a to c* show clearly that extended chain single lamellar crystals of the fractions are highly faceted. However, as reported in ref. 10, the single crystal morphology undergoes a faceting–non-faceting–refaceting process with decreasing supercooling (or increasing crystallization temperature). The morphological observations of extended chain single lamellar crystals are at the stage of the refaceting process. Detailed descriptions and discussions of this phenomenon will appear elsewhere<sup>26</sup>.

## DISCUSSION

We start our discussion by applying nucleation theory to low molecular mass PEO and MPEO fractions where entanglement is non-existent<sup>27</sup>. In the past, detailed calculations of the growth flux for  $C_{24}H_{50}$  and  $C_{26}H_{54}$  and mixtures thereof<sup>28</sup>, using the Lauritzen–DiMarzio–Passaglia formalism<sup>29</sup>, indicated that the crystal growth rate ( $G$ ), in regime I, varies almost exactly linearly with supercooling ( $\Delta T$ ) in the region where  $\Delta T$  is small. Linear relationships between  $G$  and  $\Delta T$  are also observed in the low molecular mass pure *n*-alkanes, as well as fractions of PE, PEO and MPEO cases. In Hoffman's treatment<sup>11,22</sup> for the growth rate of extended chain crystals, the growth rate was predicted to be of the form  $G = K(T_o - T_c)$  where  $K$  is the slope,  $T_c$  is the isothermal crystallization temperature and  $T_o$  is near  $T_m$  for a pure material and below  $T_m$  for a fraction<sup>11</sup>. For the cases of PEO and MPEO fractions,  $T_o$  is obtained by extrapolating the growth rate to zero, and should be representative of the melting temperature of an isolated lamella. The melting temperature of PEO and MPEO fractions listed in *Table 1* are our observations of the melting of isolated extended chain single lamellae; we thus write, in a formulation for regime I

growth<sup>11,22</sup>:

$$\begin{aligned}
 G(I) = & N_o b_o (kT/h) \exp[\psi a_o b_o l_o (1 - \gamma) \Delta G / (kT)] \\
 & \times \exp[-Q_D^* / (RT)] \exp[-2b_o l_o (1 - \gamma) \sigma / (kT)] \\
 & \times \exp[-2a_o b_o \sigma' / (kT)] \\
 & \times [1 - \exp\{-[a_o b_o l_o (1 - \gamma) \Delta G - 2a_o b_o \sigma'] / (kT)\}]
 \end{aligned} \quad (1)$$

Here  $a_o$  and  $b_o$  are dimensions of the cross-section of a single chain molecule;  $N_o$  is the number of reacting species (assumed to equal  $C_o n_s$ , where  $C_o$  is a numerical constant and  $n_s$  the number of stems in the substrate);  $l_o$  represents an average extended chain length in a fraction;  $Q_D^*$  is the diffusional activation energy;  $\Delta G$  is the Gibbs free energy for crystallization;  $\sigma'$  is the transient surface free energy associated with the two chain-end type surfaces exposed to the melt;  $\sigma$  is the transient lateral surface free energy;  $R$ ,  $k$  and  $h$  are the gas, Boltzmann and Planck constants, respectively. Of particular interest,  $\psi$  is an apportionment factor for the attachment of chain repeating units during crystal growth, the value of which is proportional to the ratio of  $n^*/n$ , where  $n^*$  is the number of crystallographic repeating unit (segment) attachments per chain molecule in the activated complex, and  $n$  is the number of total repeating units in the chain. Assuming  $n^* = 7$  leads to a range of  $\psi$  values from 0.10 for MW = 3000 to 0.04 for MW = 7100. The origin of  $\gamma$  is from comparison of the actual length of the chain involving  $\sigma$  in nucleus formation with the average extended chain length,  $l_o$ . A range of 0.1–0.2 for  $\gamma$  can be estimated using experimental observations from time-resolved small-angle X-ray scattering (SAXS) as shown in Figures 8 and 10 of refs 8 and 9, as well as recent synchrotron SAXS data<sup>26</sup>. In regime II growth, the term on the right-hand side of equation (1),  $\exp[-2b_o l_o (1 - \gamma) \sigma / (kT)]$ , is replaced by  $\exp[-b_o l_o (1 - \gamma) \sigma / (kT)]$ . The pre-exponent term is also different<sup>22</sup>.

Since we are discussing the extended chain crystal growth of low molecular mass PEO and MPEO fractions at low supercoolings, the linear relationship between  $G$  and  $\Delta T$  is associated almost exclusively with the last term (in  $[1 - \exp X]$ ) on the right-hand side of equation (1). On the other hand, the leading term,  $\exp[\psi a_o b_o l_o (1 - \gamma) \Delta G / (kT)]$ , is close to unity due to the small value of  $\psi$ . Therefore, one can obtain the slope of the relationship between  $G$  and  $\Delta T$  in regime I as

$$\begin{aligned}
 K = & N_o b_o (kT/h) W \exp[-Q_D^* / (RT)] \\
 & \times \exp[-2b_o l_o (1 - \gamma) \sigma / (kT)] \\
 & \times \exp[-2a_o b_o \sigma' / (kT)]
 \end{aligned} \quad (2)$$

where

$$W = a_o b_o l_o (1 - \gamma) (\Delta h_f) / [(kT) T_m] \quad (3)$$

and  $\Delta h_f$  is the heat of fusion. Correspondingly, if the growth is in regime II, the second exponential term on the right-hand side of equation (2) should be changed to  $\exp[-b_o l_o (1 - \gamma) \sigma / (kT)]$ . The pre-exponential term should also be different; however, this is not important in our treatment since only ratios of the two slopes are interesting (see below).

When one compares the slopes for a PEO and an MPEO fraction with the same molecular length (the same  $l_o$ ), a much simplified formulation of the ratio between two slopes can be achieved based on the assumptions

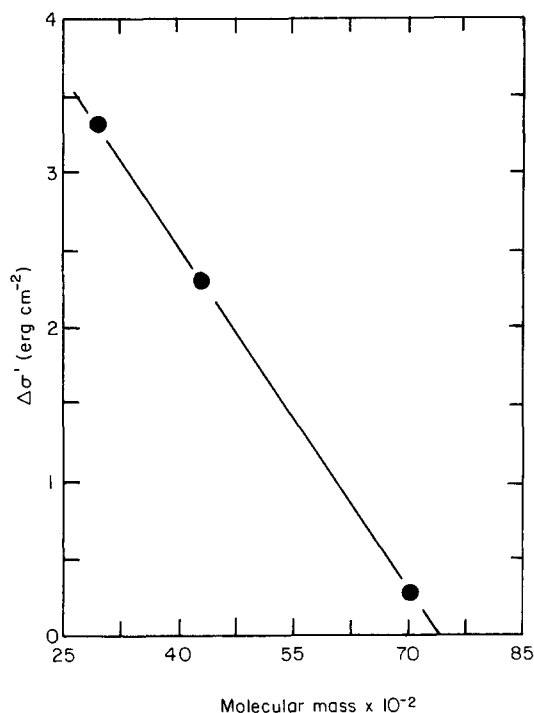


Figure 7 Relationship between the difference of transient end surface free energies,  $\Delta\sigma'$  and molecular mass of PEO fractions

that the parameters  $a_o$ ,  $b_o$ ,  $N_o$ ,  $\Delta h_f$ ,  $Q_D^*$ ,  $\sigma$  and  $\gamma$  are essentially unchanged:

$$K(\text{PEO})/K(\text{MPEO}) = \exp[-2a_o b_o \Delta\sigma' / (kT)] \quad (4)$$

where  $\Delta\sigma' = \sigma'(\text{PEO}) - \sigma'(\text{MPEO})$ . The reason for different  $\sigma'$  values in these two fractions is recognized in the experimental observations of different self-diffusion coefficients and melt viscosities<sup>9</sup>. This phenomenon has been attributed to an end group effect in these fractions since low molecular mass PEO fractions with hydroxyl end groups can form hydrogen bonding not only in the solid state, but also in the melt<sup>9,10</sup>. This association in the melt may lead to increasingly rough chain-end crystal surfaces which involve more kinetic ciliation<sup>22</sup> compared with those of MPEO fractions which have no hydrogen bonding associations. This is expected since attachment of the segments during the crystal growth is basically a blind process until well after their neighbours are crystallized. One can thus obtain different  $\sigma'(\text{PEO})$  and  $\sigma'(\text{MPEO})$  during transient crystal growth even though their molecular lengths are the same.

Although the values of  $\Delta\sigma'$  for PEO and MPEO fractions with the same molecular lengths can be calculated through equation (4), the absolute values of  $\sigma'$  for each fraction are still unavailable. However, it is clear that the calculated value of  $\Delta\sigma'$  decreases almost linearly with increasing molecular length, as shown in Figure 7. This indicates that at a sufficiently high molecular length, for PEO and MPEO fractions with the same molecular lengths, the roughness of chain-end crystal surfaces involving the end groups becomes more or less the same, and therefore,  $\Delta\sigma' = 0$ . From Figure 7, an extrapolation indicates that  $\Delta\sigma' = 0$  should be observed above MW  $\approx$  7460. Self-diffusion coefficient measurements<sup>27</sup>, obtained using a pulsed-gradient spin-echo nuclear magnetic resonance method, show that the critical molecular mass of PEO fractions at the onset of entangled behaviour, necessary for reptative transport,

is in the vicinity of MW = 7200. Earlier shear viscosity measurements of molten PEO fractions<sup>20</sup> also showed that chain entanglements occur for MW > about 7000. Therefore, it is reasonable to speculate that the difference between PEO and MPEO fractions due to chain end effect vanishes at the molecular mass required for the onset of chain entanglement. In other words, the chain entanglement effect becomes a more dominant phenomenon than hydrogen bonding association during the crystal growth. This is logical since as soon as at least one chain entanglement (net) per chain is formed, the disentanglement process during the crystal growth must occur through reptational motion.

On the other hand, one can also compare the slopes between two PEO (or two MPEO) fractions with the same end groups, but different molecular lengths. In this case, the ratio between two slopes can be written as:

$$\begin{aligned} K(1)/K(2) &= l_o(1)T_m(2)/[l_o(2)T_m(1)] \\ &\times \exp[-2b_o\Delta l_o(1-\gamma)\sigma/(kT)] \\ &\times \exp[-2a_ob_o\Delta\sigma'_o/(kT)] \end{aligned} \quad (5)$$

where 1 and 2 represent two PEO (or MPEO) fractions with different molecular lengths,  $\Delta l_o = l_o(1) - l_o(2)$ , and  $\Delta\sigma'_o = \sigma'(1) - \sigma'(2)$ . The other assumptions applied to equation (4) still hold. In particular, the diffusional activation energies for the different molecular lengths studied are unchanged<sup>9,27</sup>. The values of  $\gamma(1)$  and  $\gamma(2)$  are assumed to be equal and simplified as  $\gamma$ . Again, for regime II growth, the term of  $\exp[-2b_o\Delta l_o(1-\gamma)\sigma/(kT)]$  in equation (5) is replaced by  $\exp[-b_o\Delta l_o(1-\gamma)\sigma/(kT)]$ . In this equation two unknown parameters,  $\sigma$  and  $\Delta\sigma'_o$ , exist. The value of  $\sigma$  can be calculated only after one assumes a reasonable value for  $\Delta\sigma'_o$ . Therefore, an independent way to estimate  $\Delta\sigma'_o$  is necessary.

Here we test the statistical mechanical calculations for  $\Delta\sigma'_o$  originally proposed by Lauritzen and DiMarzio<sup>30</sup>, and recently extended by Hoffman<sup>22</sup>. Based on their formulation, the transient chain-end surface free energy associated with the cilia on one end of the nucleus is:

$$\sigma' = \lambda[kT/(a_ob_o)]\{\ln[l_{cil(max)}/x_o] - 1\} \quad (6)$$

where  $l_{cil(max)}$  represents a maximum contour length attached onto a crystal surface, and  $x_o$  is the statistical segment length such that  $l_{cil(max)}/x_o$  is the maximum number of statistical chain units in the cilium. The value of  $\lambda = \pi/2\phi$  is dependent upon the angle of sweep of the cilium,  $\phi$ . The value of  $\Delta\sigma'_o$  for two particular fractions can thus be calculated as:

$$\begin{aligned} \Delta\sigma'_o &= \lambda[kT/(a_ob_o)] \\ &\times \ln\{l_{cil(max)}(1)x_o(2)/[l_{cil(max)}(2)x_o(1)]\} \end{aligned} \quad (7)$$

If one adopts the average transient folding length from SAXS experimental data<sup>7-10,26,31</sup> as equal to  $2l_{cil(max)} + n^*$ ,  $\lambda \simeq 0.5$ , and  $x_o(1) = x_o(2)$ , the calculated value of  $\Delta\sigma'_o$  for MPEO(MW = 4250) and MPEO(MW = 3000) is in a range of 2.4–3.4 erg cm<sup>-2</sup>\*; that for MPEO(MW = 7100) and MPEO(MW = 4250) is in a range of 3.5–4.6 erg cm<sup>-2</sup>; and that for MPEO(MW = 7100) and MPEO(MW = 3000) is in a range of 6.4–7.5 erg cm<sup>-2</sup>. For their PEO counterparts, values of  $\Delta\sigma'_o$  are in ranges of 1.5–2.5 erg cm<sup>-2</sup>, 1.7–2.7 erg cm<sup>-2</sup> and 3.5–4.5 erg cm<sup>-2</sup>, respectively.

The differences of the calculated  $\Delta\sigma'_o$  between the pairs

of MPEO from that of PEO fractions are caused by the differences of the average transient folding lengths observed from SAXS measurements<sup>7-10,26,31</sup>. It should be pointed out that the calculations carried out based on equation (7) have some degree of variability because of the uncertainties in  $l_{cil(max)}$ ,  $\lambda$  and the precise value of  $x_o$ . Nevertheless, if one compares the data with the calculations of  $\Delta\sigma'$  based on equation (4), one finds that they are consistent.

Substituting these  $\Delta\sigma'_o$  values into equation (5), one can calculate the transient lateral surface free energy  $\sigma$  for PEO and MPEO fractions. All the results fall into a range of  $\sigma = 1.0$ –1.2 erg cm<sup>-2</sup>. No molecular length dependence on  $\sigma$  can be observed. This range is about one order of magnitude smaller than the value generally accepted<sup>4,32</sup>. The reason for such a small transient lateral surface free energy may be attributed to the highly serrated (1 0 0) crystallographic planes (see below). This calculation, in turn, supports our assumption that  $\sigma$  is constant in the fractions when we derived equation (4). If the crystal growth is in regime II, the transient lateral surface free energy lies between 2.0 and 2.4 erg cm<sup>-2</sup>.

It is also worthwhile to further study equations (1) and (2) based on the absolute reaction treatment<sup>33</sup>, which was adopted to find crystal growth rates controlled by surface nucleation<sup>15-19</sup>. The total flux across the nucleation barrier is given by the relation<sup>34,35</sup>:

$$S_T = N_oA_o(A - B)/(A - B + B_1) = N_oA_o(1 - B/A) \quad (8)$$

The second equality holds when the rate of backward reactions (removal)  $B$  is the same as the rate of the backward reaction of the first stem  $B_1$ . In regime I, the crystal growth rate can be written as<sup>19,36</sup>:

$$G(I) = b_oS_T = N_ob_oA_o(1 - B/A) \quad (9)$$

Note that  $(1 - B/A)$  is the only term related to supercooling  $\Delta T$ . At very low supercoolings, the backward reaction rate is close to, but still slightly smaller than, the forward reaction rate. Thus, the term  $(1 - B/A)$  is close to zero. At a temperature where  $A = B$ , the crystal growth rate  $G = 0$  for a finite value of  $A_o$ . This temperature is therefore the equilibrium melting temperature. Furthermore, the lower activity of the backward reaction with increasing supercooling leads to a  $G = K\Delta T$  growth in this temperature region. In equation (9) the value of  $A_o$  is the slope of crystal growth rate with respect to supercooling,  $dG/d(\Delta T)$ , which is equivalent to the slope  $K$  expressed by equation (2). As listed in Table 2, it is evident that with increasing molecular length the value of  $A_o$  decreases exponentially. This indicates that the forward reaction rate of the first stem is drastically hampered with increasing molecular length. Such an increase of the nucleation barrier is mainly caused by a rise in  $\sigma'$  with molecular length, and therefore is entropic in nature. However, the barrier ( $A_o$ ) for each fraction does not change in this temperature region during the crystal growth.

Turning to morphological aspects, we have a unique opportunity to observe the change of single lamellar crystal morphologies in these PEO and MPEO fractions. This requires explanations involving molecular considerations. An attempt was carried out by Sadler<sup>6</sup> who stated that all the single lamellar crystals of low molecular mass PEO fractions grown from the melt are above the temperature where the equilibrium roughening transition

\*1 erg =  $1 \times 10^{-7}$  J

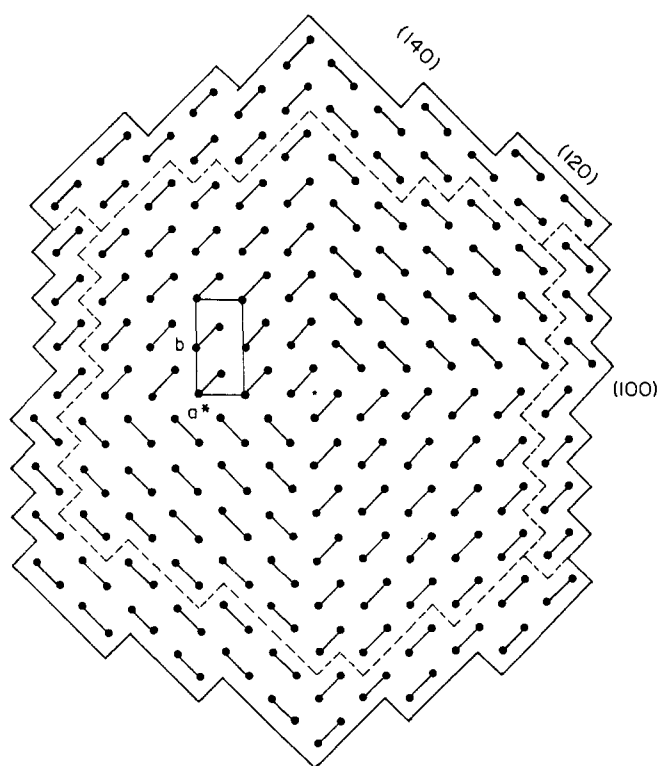


**Figure 8** PEO molecular crystal packing model with  $a^* = \alpha \sin \beta = 0.656$  nm and  $b = 1.304$  nm

occurs. This transition is characterized by a morphological change from a faceted single crystal to a curved one, such as in the case of PE crystallized from dilute solution<sup>37</sup>. Therefore, according to Sadler's description, the straightness of the crystallographic planes observed in low molecular mass PEO and MPEO fractions is coincidental and not the outcome of faceting<sup>6</sup>. Any change of the morphology observed<sup>1-5,10,26,31</sup> in the single lamellar crystals is a cause of 'kinetic effects'. Naturally, this kind of explanation leads to his rough surface growth model<sup>38,39</sup>, which describes polymer crystal growth either without a nucleation barrier ( $G \propto \Delta T$ ) or with an entropic barrier [ $\log G \propto 1/(T\Delta T)$ ].

It is well known that, in general, surface nucleation-controlled growth proceeds anisotropically, responding less readily to its growth-driving force ( $\Delta G$ ). Growth habits of a single crystal are bounded by the slowest growing crystallographic planes. The size of the resulting 'facets' however, depends upon the Gibbs free energy gradient and its orientation with respect to the lattice. On the other hand, rough surface growth responds to very small gradients in the driving force, and the growth proceeds isotropically. As a consequence, the shape of a growing single crystal surface is a true replica of the temperature or concentration profile in the melt or solution. This is reflected in a macroscopically rounded growth front. Nevertheless, the absence of macroscopic facets in parts of a curved crystal surface does not necessarily imply that rough surface growth prevails there.

For PEO single lamellar crystals grown from the melt, Kovacs and Straupe<sup>4</sup> proposed a molecular crystal packing in a single lamellar crystal, as shown in Figure 8. In this model, the folds are supposedly parallel to the  $\{1\ 2\ 0\}$  planes as in solution-grown crystals<sup>40</sup>. Though  $(1\ 0\ 0)$  folds may also be conceived in the  $(1\ 0\ 0)$  sectors,

folds parallel to  $\{1\ 4\ 0\}$  planes are unrealistic since they would involve a fold packing which is too dense in the corresponding sectors. On a molecular scale, one can see from Figure 8 that the growth faces of the PEO single lamellar crystals are more highly serrated, rather than being smooth. Nevertheless, the density of niches along the  $\{1\ 4\ 0\}$  planes is about half of the niche density along the  $(1\ 0\ 0)$  planes. In the cases of extended chain crystals discussed, the growth along  $\{1\ 4\ 0\}$  planes is slower than that along  $(1\ 0\ 0)$  planes for PEO (MW = 3000) and MPEO (MW = 3000) fractions. This is documented by an aspect ratio of 0.8, as shown in Figures 4 and 6. This value corresponds well to the observation that the growth along  $(1\ 0\ 0)$  planes is twice as fast as that along  $\{1\ 4\ 0\}$  planes. This can be understood by the ratio of niche densities along these two crystallographic planes if every niche becomes growth-active. With increasing molecular length, the aspect ratio increases to close to unity, or even slightly higher than one (Figures 4 and 6). Basically, the growth rates along two directions are thus almost equal. This observation has also been supported by Kovacs's data<sup>1-5</sup>. For example, the aspect ratio was found to be 0.8 for PEO (MW = 2780) fraction crystallized at  $T_c = 328.2$  K ( $\Delta T = 2.6$  K); 0.84 for PEO (MW = 3900) fraction crystallized at  $T_c = 331.2$  K ( $\Delta T = 2.4$  K); and around or slightly higher than unity for PEO (MW = 5970) fraction in the temperature region where the extended chain crystals grow. It seems that along the  $(1\ 0\ 0)$  planes, only half or even slightly less than half of the niches are growth-active. We speculate that with increasing molecular length, attachment of extended chain conformations onto a crystal surface becomes increasingly difficult. Attachments with non-integral folded chain conformations are more favourable. The final extended chain crystal may form through an isothermal thickening process on the crystal surface during growth. However, direct experimental observations of this phenomenon are still awaited.

## CONCLUSION

The crystal growth of extended chain single lamellar crystals in low molecular mass PEO and MPEO fractions near their melting temperatures show a linear relationship between  $G$  and  $\Delta T$ . This indicates that the nucleation barrier during growth is not changed for a constant molecular length. This barrier is exponentially dependent upon the molecular length. The growth rate is thus affected by a compromise between forward (attachment) and backward (removal) reactions which are dependent on  $\Delta T$ . Based on recent development of the nucleation theory<sup>11,22</sup>, the transient lateral surface free energy,  $\sigma$ , is calculated to be in a range of  $1.0$ – $1.2$  erg  $\text{cm}^{-2}$  if the crystal growth is in regime I. This value increases to  $2.0$ – $2.4$  erg  $\text{cm}^{-2}$  when regime II growth is assumed. The differences between transient chain-end surface free energies for fractions of PEO and MPEO with the same molecular lengths as well as for two PEO or two MPEO fractions with different molecular lengths are also estimated. They are certainly chain end group- and molecular length-dependent. These surface free energies possess entropic origins. Morphological aspects of the single lamellar chain crystals can also be correlated with crystal growth on a molecular scale. However, some assumptions made in this approach still need to be examined by further experiments.

## ACKNOWLEDGEMENTS

This research was partially supported by the Exxon Educational Foundation. One of the authors (S.Z.D.C.) would like to express his gratefulness to Professor Hoffman who provided the preprint of his recent work on the nucleation theory to describe the crystal growth of *n*-alkanes.

## REFERENCES

- 1 Kovacs, A. J. and Gonthier, A. *Kolloid Z. Z. Polym.* 1972, **250**, 530
- 2 Kovacs, A. J., Gonthier, A. and Straupe, C. *J. Polym. Sci., Polym. Symp.* 1975, **50**, 283
- 3 Kovacs, A. J., Straupe, C. and Gonthier, A. *J. Polym. Sci., Polym. Symp.* 1977, **59**, 31
- 4 Kovacs, A. J. and Straupe, C. *J. Chem. Soc. Faraday Discuss.* 1979, **68**, 225
- 5 Kovacs, A. J. and Straupe, C. *J. Crystal Growth* 1980, **48**, 210
- 6 Sadler, D. M. *J. Polym. Sci., Polym. Phys. Edn* 1985, **23**, 1533
- 7 Cheng, S. Z. D., Zhang, A.-Q. and Chen, J.-H. *J. Polym. Sci., Polym. Lett.* 1990, **28**, 233
- 8 Cheng, S. Z. D., Zhang, A.-Q., Chen, J.-H. and Heberer, D. P. *J. Polym. Sci., Polym. Phys. Edn* 1991, **29**, 287
- 9 Cheng, S. Z. D., Chen, J.-H., Zhang, A.-Q. and Heberer, D. P. *J. Polym. Sci., Polym. Phys. Edn* 1991, **29**, 299
- 10 Cheng, S. Z. D. and Chen, J.-H. *J. Polym. Sci., Polym. Phys. Edn* 1991, **29**, 311
- 11 Hoffman, J. D. *Macromolecules* 1985, **18**, 772
- 12 Leung, W. M., St. John Manley, R. and Panaras, A. R. *Macromolecules* 1985, **18**, 746
- 13 Leung, W. M., St. John Manley, R. and Panaras, A. R. *Macromolecules* 1985, **18**, 753
- 14 Leung, W. M., St. John Manley, R. and Panaras, A. R. *Macromolecules* 1985, **18**, 760
- 15 Lauritzen Jr, J. I. and Hoffman, J. D. *J. Res. Natl. Bur. Stand. Sect. A* 1960, **64**, 73
- 16 Lauritzen Jr, J. I. and Hoffman, J. D. *J. Appl. Phys.* 1973, **44**, 4340; 4353
- 17 Frank, F. C. and Tosi, M. *Proc. R. Soc. London Ser. A* 1961, **263(A)**, 323
- 18 Frank, F. C. *J. Crystal Growth* 1974, **22**, 233
- 19 Hoffman, J. D., Davis, G. T. and Lauritzen Jr, J. I. in 'Treatise on Solid State Chemistry', Vol. 3 (Ed. N. B. Hannay), Plenum, New York, 1976, Ch. 7, pp. 497-614
- 20 Point, J. J. and Kovacs, A. J. *Macromolecules* 1980, **13**, 399
- 21 Hoffman, J. D. *Macromolecules* 1986, **19**, 1124
- 22 Hoffman, J. D. *Polymer* in press
- 23 Ungar, G. and Keller, A. *Polymer* 1987, **28**, 1899
- 24 Organ, S. J., Ungar, G. and Keller, A. *Macromolecules* 1989, **22**, 1995
- 25 Cooper, D. R. and Booth, C. *Polymer* 1977, **18**, 164
- 26 Cheng, S. Z. D., Chen, J.-H., Zhang, A.-Q., Barley, J. S., Habenschuss, T. and Zschack, P. in preparation
- 27 Cheng, S. Z. D., Barley, J. S. and von Meerwall, E. D. *J. Polym. Sci., Polym. Phys. Edn* 1991, **29**, 515
- 28 Lauritzen Jr, J. I., Passaglia, E. and DiMarzio, E. A. *J. Res. Natl. Bur. Stand. Sect. A* 1967, **71**, 245
- 29 Lauritzen Jr, J. I., DiMarzio, E. A. and Passaglia, E. *J. Chem. Phys.* 1966, **45**, 444
- 30 Lauritzen Jr, J. I. and DiMarzio, E. A. *J. Res. Natl. Bur. Stand.* 1978, **83**, 381
- 31 Chen, J.-H. PhD Dissertation, The University of Akron, 1992
- 32 Cheng, S. Z. D., Chen, J.-H. and Janimak, J. J. *Polymer* 1990, **31**, 1081
- 33 Turnbull, D. and Fisher, J. C. *J. Chem. Phys.* 1949, **17**, 71
- 34 Frank, F. C. and Tosi, M. *Proc. R. Soc. London* 1960, **263A**, 323
- 35 Gornick, F. and Hoffman, J. D. *Ind. Eng. Chem.* 1966, **58**(2), 41
- 36 Hoffman, J. D. *Polymer* 1982, **23**, 656
- 37 Organ, S. J. and Keller, A. *J. Polym. Sci., Polym. Phys. Edn* 1986, **24**, 2319
- 38 Sadler, D. M. *Polymer* 1983, **24**, 1401
- 39 Sadler, D. M. *Polymer* 1987, **28**, 1440
- 40 Lotz, B., Kovacs, A. J., Basset, G. A. and Keller, A. *Kolloid Z. Z. Polym.* 1966, **209**, 115